

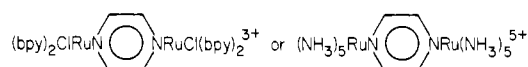
Outer-Sphere Charge Transfer in Mixed-Metal Ion Pairs¹

JEFF C. CURTIS and THOMAS J. MEYER*

Received August 19, 1981

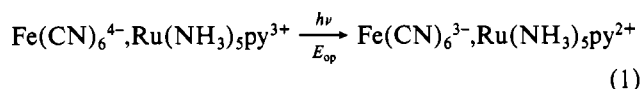
Outer-sphere charge-transfer (OSCT) transitions have been observed in water for a series of mixed-metal ion pairs: $[M^{II}(\text{CN})_6, \text{Ru}^{III}(\text{NH}_3)_5(\text{L})]^-$ ($M = \text{Fe}, \text{Ru}, \text{Os}$; $\text{L} = \text{pyridine}$ or a substituted pyridine). After developing an appropriate thermochemical cycle it is possible to show that as expected from theory, the energies of the optical transitions vary with $\Delta H_{\text{IP}}^{\text{opt}}$ where $\Delta H_{\text{IP}}^{\text{opt}}$ is the enthalpy difference associated with charge transfer within the ion pair, $[M^{II}(\text{CN})_6, \text{Ru}^{III}(\text{NH}_3)_5(\text{L})]^- \rightarrow [M^{III}(\text{CN})_6, \text{Ru}^{II}(\text{NH}_3)_5(\text{L})]^-$. A detailed analysis of the OSCT absorption bands leads to a number of important conclusions, including (1) the presence of electronic structure is due to the effects of spin-orbit coupling at the $M^{III}(\text{CN})_6^{3-}$ d^3 core following optical excitation, (2) the extent of electronic coupling between electron-donor and -acceptor sites is only slightly dependent on M in $M(\text{CN})_6^{4-}$, and (3) the most probable outer-sphere "structure" involves contact between $M(\text{CN})_6^{4-}$ and an ammine face of the complexes $\text{Ru}(\text{NH}_3)_5(\text{L})^{3+}$.

In mixed-valence ions such as



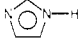
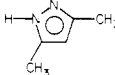
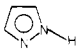
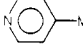
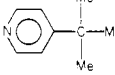

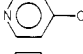
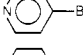
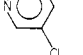
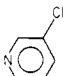
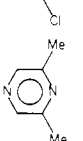
(bpy = 2,2'-bipyridine), the observation of low-energy inter-valence transfer (IT) or metal-metal charge-transfer (MMCT) absorption bands has been of great value in providing experimental information on a number of important issues including (1) a description of electronic structure,¹⁻³ (2) relationships between optical and thermal electron transfer,³⁻⁶ and (3) the role of solvent in charge-transfer processes.⁷ It is an area that has been especially notable for the interplay between theory and experiment.⁸

One issue of importance to evolve from the work on mixed-valence ions is the possibility of extensions of the basic ideas and formalisms in a more general way to charge-transfer processes in chemical systems. In an earlier communication we reported the appearance of an outer-sphere charge transfer (OSCT) band in solution for the ion pair $\text{Fe}(\text{CN})_6^{4-}, \text{Ru}(\text{NH}_3)_5\text{py}^{3+}$ (py is pyridine) (eq 1).⁹ We have now completed



studies on an extended series of closely related ion pairs and present here our findings in detail. The ion pairs are an interesting case since they allow the ideas developed for mixed-valence dimers to be extended to charge transfer in outer-sphere cases. Although OSCT bands should be observable in association complexes such as $\text{Fe}(\text{H}_2\text{O})_6^{2+}, \text{Fe}(\text{H}_2\text{O})_6^{3+}$, their equilibrium concentrations are no doubt so low as to make the experiment impractical. Using unlike charged ions has the advantage of introducing an attractive, electrostatic binding between the ions which allows the observation of OSCT absorption bands.

Table I. Structures, Names, and Abbreviations of the Various Ligands Employed in This Study

ligand	name	abbreviation
	imidazole	Im
	2,5-dimethylpyrazole	Me ₂ pzl
	pyrazole	pzl
	4-methylpyridine	4-Mepy
	4-tert-butylpyridine	4- <i>t</i> -Bupy
	pyridine	py
	4-chloropyridine	4-Cl(py)
	4-bromopyridine	4-Br(py)
	3-chloropyridine	3-Cl(py)
	3,5-dichloropyridine	3,5-Cl ₂ py
	3,5-dimethylpyrazine	3,5-Me ₂ pz

Experimental Section

Materials and Apparatus. Deionized water was distilled once from KMnO_4 . Electrochemical measurements were performed on a PAR 173 potentiostat using a house-designed signal generator and a Hewlett-Packard 7015B X-Y chart recorder. Electronic spectra were obtained on a Cary 17 recording spectrophotometer.

All electrochemical and spectrophotometric experiments were performed in a medium of 0.10 M ionic strength buffered to pH 5. This medium consisted of 0.09 M sodium trifluoroacetate (Aldrich) and a pH 5 sodium acetate/acetic acid buffer of 0.01 M ionic strength formulated according to the nomogram of Boyd.¹⁰ These solutions were stable with regard to pH for several weeks. For sensitive spectrophotometric experiments, the solutions were filtered through a fine sintered glass frit just prior to use so as to remove any dust

- (1) Taken from: Curtis, J. C., Ph.D. Dissertation, The University of North Carolina, 1980.
- (2) Taube, H. *Ann. N.Y. Acad. Sci.* **1978**, *313*, 483.
- (3) (a) Hush, N. S. *Prog. Inorg. Chem.* **1967**, *8*, 391; *Electrochim. Acta* **1968**, *13*, 1005; *Chem. Phys.* **1975**, *10*, 361. (b) Robin, M. B.; Day, P. *Adv. Inorg. Chem. Radiochem.* **1967**, *10*, 247.
- (4) Creutz, C. *Inorg. Chem.* **1978**, *12*, 3723. Tom, G. M.; Creutz, C.; Taube, H. *J. Am. Chem. Soc.* **1974**, *96*, 7827.
- (5) Meyer, T. J. In "Mixed Valence Compounds"; Brown, D. B., Ed.; 1980; pp 75-113.
- (6) Meyer, T. J. *Acc. Chem. Res.* **1978**, *11*, 94.
- (7) Sullivan, B. P.; Curtis, J. C.; Kober, E. M.; Meyer, T. J. *Nouv. J. Chim.* **1980**, *4*, 643-650.
- (8) Piepho, S. B.; Krausz, E. R.; Schatz, P. N. *J. Am. Chem. Soc.* **1978**, *100*, 2296; *Chem. Phys. Lett.* **1978**, *55*, 539.
- (9) Curtis, J. C.; Meyer, T. J. *J. Am. Chem. Soc.* **1978**, *100*, 6284.

- (10) Boyd, W. C. *J. Am. Chem. Soc.* **1945**, *67*, 1035.

Table II. Elemental Analysis Data^a

compd	calcd (obsd)		
	% C	% H	% N
K ₄ [Ru(CN) ₆]·H ₂ O	16.70 (16.80)	0 (<0.3)	19.47 (19.18)
K ₄ [Os(CN) ₆]	14.34 (14.15)	0.00 (<0.3)	16.72 (16.42)
[(NH ₃) ₅ Ru(Im)]Cl ₃ ·H ₂ O	9.51 (9.24)	5.58 (5.34)	25.88 (25.58)
[(NH ₃) ₅ Ru(Me ₂ pzl)]Cl ₃ ·3H ₂ O	13.56 (13.36)	5.69 (5.88)	22.14 (22.37)
[(NH ₃) ₅ Ru(pzl)]Cl ₃ ·2H ₂ O	9.09 (9.01)	5.83 (6.16)	24.71 (24.52)
[(NH ₃) ₅ Ru(4-Mepy)]Cl ₃ ·2H ₂ O	17.08 (16.99)	6.21 (6.01)	19.92 (19.63)
[(NH ₃) ₅ Ru(<i>t</i> -Bupy)]Cl ₃ ·3H ₂ O	22.43 (22.88)	7.10 (7.08)	17.44 (17.23)
[(NH ₃) ₅ Ru(py)]Cl ₃ ·2H ₂ O	14.73 (14.46)	5.93 (5.70)	20.61 (19.98)
[(NH ₃) ₅ Ru(4-Cl(py)))]Cl ₃ ·2H ₂ O	13.58 (13.32)	5.24 (4.69)	19.00 (19.02) ^b
[(NH ₃) ₅ Ru(4-Br(py)))]Cl ₃ ·2H ₂ O	12.30 (11.62)	4.75 (4.68)	17.26 (17.35) ^b
[(NH ₃) ₅ Ru(3-Cl(py)))]Cl ₃ ·2H ₂ O	13.58 (13.50)	5.23 (5.21)	19.00 (19.51) ^b
[(NH ₃) ₅ Ru(3,5-Cl ₂ py)]Cl ₃ ·2H ₂ O	12.13 (10.82)	4.89 (4.96)	16.98 (18.11) ^b
[(NH ₃) ₅ Ru(Me ₂ pyz)]Cl ₃	17.20 (17.87)	5.78 (5.23)	24.46 (23.79)
Li[<i>trans</i> -pyRu(NH ₃) ₄ NCRu(CN) ₅]·6H ₂ O	21.28 (21.02)	4.69 (4.00)	24.82 (24.53)

^a Analyses performed by Integral Microanalytical Laboratories, Raleigh, NC. ^b These compounds undergo significant decomposition in the solid state within 2 or 3 days of being made even when kept under vacuum.

or small amounts of particulate matter that were sometimes present due to impurities in the sodium trifluoroacetate.

Potassium ferrocyanide was purchased from Baker and Adamson and recrystallized once from H₂O. Ruthenium hexaammine trichloride and ruthenium trichloride trihydrate were purchased from Matthey Bishop and used without further purification. Potassium hexachloroosmate was purchased from Alfa-Ventron and used without further purification.

Most of the various ligands used in this study were purchased from Aldrich and used as received. Baker reagent grade pyridine was distilled once before use. The 1,3-dimethylpyrazole ligand was obtained as a gift from Dr. John Wasson.

Preparation of Complexes. Potassium ruthenocyanide, K₄[Ru^{II}(CN)₆], was synthesized according to the method of Howe by heating Ru^{III}Cl₃·3H₂O (2 g, 7.6 mmol) in 50 mL of water saturated with KCN (Baker and Adamson reagent grade) for 24 h.¹¹ Upon cooling of the solution to 0 °C, a white microcrystalline precipitate was produced. The solid material was isolated by filtration and washed extensively with methanol. The crude K₄[Ru^{II}(CN)₆] (impure with KCN) salt was purified by dissolving it in 75 mL of water at room temperature followed by the slow addition of an equal volume of methanol to precipitate the solid product. The procedure was carried out twice. Care should be taken to minimize the period of time during which the ruthenocyanide is in solution since a slow hydrolysis reaction leading to a blueish impurity does occur. The final yield after purification was generally about 60%. The analytical data for this and the other complexes used in this study are tabulated in Table II.

Potassium osminocyanide, K₄[Os^{II}(CN)₆], was synthesized and purified analogously to the ruthenium species except that the starting material was K₄[OsCl₆] and the yields were generally somewhat less—typically 40–50%.

Chloropentaammineruthenium(III) dichloride, [(NH₃)₅Ru^{III}Cl]Cl₂, was synthesized from hexaammineruthenium(III) trichloride by the method of Vogt, Katz, and Wiberly.¹² In a typical preparation, 5 g of [Ru^{III}(NH₃)₆]Cl₃ was heated at reflux in 200 mL of 6 N HCl for 8 h. Upon cooling, the crude yellow product was isolated by filtration, washed with ethanol, and dried in the air. The crude product was then recrystallized once from 0.5 N HCl. Yields after purification were 60–70%. An alternate, and much more economical, route to this complex employs the ruthenium(III) trichloride trihydrate starting material and is described in ref 13. This procedure has recently been optimized by K. A. Goldsby of these laboratories.¹⁴

Pentaammine(L)ruthenium(III) Trichloride, [(NH₃)₅Ru^{III}(L)]Cl₃. The synthesis of these systems were all carried out with use of the same procedure. The procedure is described in detail below for the case L = py (py is pyridine).

A 1.58-g (5.39-mmol) sample of [(NH₃)₅Ru^{III}Cl]Cl₂ was reduced in the presence of 4 mL (50 mmol) of pyridine and 20 mL of water over 2 g of a zinc–mercury amalgam. The reaction mixture was

slightly acidified at the outset by the addition of 1 drop of concentrated trifluoroacetic acid. This mixture was allowed to react under a blanket of argon for about 1 h, after which time the deep orange color of the [(NH₃)₅Ru^{II}py]²⁺ ion had fully developed. The solution was then filtered to remove the amalgam and other insolubles, and 5 mL of saturated NH₄PF₆ in water was added in order to precipitate the bright yellow salt [(NH₃)₅Ru^{II}py](PF₆)₂. This material was collected by filtration and dried. It was then dissolved in 50 mL of acetone, filtered to remove insolubles, and precipitated as the dichloride salt by the addition of 5 mL of a saturated solution of tetra-*n*-butylammonium chloride (Aldrich) in acetone. The dark orange material was collected by filtration and dried via several washings with 10-mL portions of anhydrous ether. The dichloride salt was then immediately dissolved in 15 mL of water and filtered (all under subdued lighting due to the known photolability of these complexes¹⁵). Oxidation to the ruthenium(III) complex was accomplished by the addition of 4 mL of a solution containing 2 mL of 30% hydrogen peroxide (Fischer Scientific Co.) and 2 mL of 2 N hydrochloric acid. The oxidation was considered to be complete after about 5 min, at which time the orange color of the [(NH₃)₅Ru^{II}py]²⁺ ion had been completely replaced by the faint yellow of the [(NH₃)₅Ru^{III}py]³⁺ ion. The crude [(NH₃)₅Ru^{III}py]Cl₃ was precipitated as a fine microcrystalline solid by the slow addition of 100 mL of acetone. This material was collected by filtration and dried. It was then recrystallized from about 50 mL of a mixture of 60% 0.05 M hydrochloric acid and 40% acetone. The crude solid was heated in this mixture to about 80 °C for 5 min and then rapidly filtered. The filtrate was cooled overnight at 0 °C and deposited beautiful yellow needles of [(NH₃)₅Ru^{III}py]Cl₃. Precipitation could then be enhanced by the slow addition of another 10–15 mL of acetone. The yield was 1.4 g (64%). Microanalytical data for this and the other complexes synthesized by this method are tabulated in Table II. For those ligands which were not readily soluble in water such as 4-*tert*-butylpyridine, 4-methylpyridine, and 3,5-dichloropyridine, the initial reduction step was carried out with 2 or 3 mL of acetone present so as to enhance the solubility of the ligand. These reactions, however, typically went rather less cleanly and gave lesser yields (30–40%) than the more straightforward cases where L was readily water soluble.

***trans*-Tetraammine(pyridine)(sulfato)ruthenium(III) chloride, *trans*-[pyRu^{III}(NH₃)₄SO₄]Cl**, was synthesized according to the method of Isied and Taube¹⁶ with the [*trans*-ClRu^{II}(NH₃)₅SO₂]Cl starting material made according to the method developed by Clarke and Ford.¹³

***trans*-Tetraammine(pyridine)ruthenium(III) Ruthenicyanide (Lithium Salt), Li[*trans*-pyRu^{III}(NH₃)₄NCRu^{II}(CN)₅]**. This material was synthesized by simply mixing 0.107 g of [*trans*-pyRu^{III}(NH₃)₄SO₄]Cl (0.31 mmol) and 0.25 g of K₄[Ru^{II}(CN)₆] (0.58 mmol) together in 3 mL of neutral water and allowing the mixture to stand for 48 h in the dark. The resulting dark blue mixture of the dimeric anion [*trans*-pyRu^{III}(NH₃)₄NCRu^{II}(CN)₅]⁻ and the trimeric cation [*trans*-pyRu^{III}(NH₃)₄NCRu^{II}(CN)₄CNRu^{III}(NH₃)₄py]²⁺ was then

(11) Howe, J. L. *J. Am. Chem. Soc.* **1980**, *102*, 981.

(12) Vogt, L. H.; Katz, J. L.; Wiberly, S. E. *Inorg. Chem.* **1965**, *4*, 1156.

(13) Clarke, R. E. Masters Thesis, University of California at Santa Barbara, 1969.

(14) Goldsby, K. A., unpublished work.

(15) Malouf, G.; Ford, P. C. *J. Am. Chem. Soc.* **1977**, *99*, 7213.

(16) Isied, S.; Taube, H. *Inorg. Chem.* **1974**, *13*, 1545; **1976**, *15*, 3070.

slowly run through a 50-mL column of J. T. Baker chromatographic grade CGC241 200–400 mesh cation-exchange resin in the Li^+ form. The cationic trimer stuck at the top as a dark blue band, and the dimeric species washed through unaffected. The crude $\text{Li}[\text{trans-pyRu}^{\text{III}}(\text{NH}_3)_4\text{NCRu}^{\text{II}}(\text{CN})_5]$ was isolated by the addition of 100 mL of methanol followed by filtration through a fine sintered glass frit. The LiSO_4 and $\text{Li}_4[\text{Ru}^{\text{II}}(\text{CN})_6]$ contaminants were removed by dissolving the solid in a small volume of water (~ 3 mL) and then adding several drops of a saturated solution of bis(diphenylphosphonium) chloride (PPN), $[\text{Ph}_2\text{PCPPH}_2]\text{Cl}_2$ (Aldrich), in water. The white precipitate was then separated from the blue solution by filtration, and the purified product was isolated by dropping the blue liquid into 100 mL of stirring methanol. This procedure was repeated until the PPN precipitate was substantially blue in color, at which point the purification was judged complete. The yield after purification was typically 20–30%. Anal. Calcd for $\text{Li}[\text{Ru}(\text{CN})_5\text{CNRu}(\text{NH}_3)_4\text{py}]\cdot 6\text{H}_2\text{O}$: C, 21.28; H, 4.60; N, 24.82. Found: C, 21.02; H, 4.00; N, 24.53.

The trimeric species $[\text{pyRu}^{\text{III}}(\text{NH}_3)_4\text{NCRu}^{\text{II}}(\text{CN})_4\text{CNRu}^{\text{III}}(\text{NH}_3)_4\text{py}]\text{Cl}_2$ could be isolated by adjusting the starting ratio of the ammine to the hexacyanide complex to 1:1 and substituting Baker chromatographic grade CGA-316 200–400 mesh anion-exchange resin in the chloride form for the cation resin used above. In this case the anionic dimer remained as a blue band at the top while the trimer came through with the eluent (water). This material could be isolated by dropping it into a large volume of either methanol or acetone.

It was found that ferrocyanide could be successfully substituted for ruthenocyanide in the above procedures (and so, presumably, could osminocyanide).

Results

Reduction Potentials. Electrochemical measurements were carried out with both gold and glassy-carbon disk electrodes which were freshly polished before each experiment. All potentials are referenced to the SCE. The results are shown in Table III for the various complexes used in this study. In the cyclic voltammetry experiments the $E_{1/2}$ value was taken as the midpoint potential between the oxidative and reductive peak maximum at 200 mV/s sweep rates (differences in diffusion coefficients between the oxidized and reduced species were assumed small).

The $[(\text{NH}_3)_5\text{Ru}^{\text{III}}(\text{L})]^{3+/2+}$ couples displayed quasi-reversible waves (in the electrochemical sense) on the gold electrode ($\Delta E_{\text{peak}} = 70\text{--}100$ mV) and somewhat irreversible waves on glassy carbon ($\Delta E_{\text{peak}} = 100\text{--}150$ mV). However, the $E_{1/2}$ values obtained agree quite well between the different electrodes.

The $[\text{M}^{\text{II/III}}(\text{CN})_6]^{4-/3-}$ couples displayed significantly irreversible electrochemical waves on both gold ($\Delta E_{\text{peak}} = 500\text{--}600$ mV) and glassy carbon ($\Delta E_{\text{peak}} = 180\text{--}300$ mV). In the case of ferrocyanide, for example, the average of the $E_{1/2}$ values obtained on gold and carbon of $+0.187 \pm 0.010$ V is in reasonable agreement with the values available in the literature (≈ 0.17 V at pH 2 according to ref 17; 0.22 V at pH 12 according to ref 18) and the value obtained via differential pulse polarography on glassy carbon of 0.187 V (obtained at 5 mV/pulse modulation amplitude and 1.0 mV/s scan rate). In the differential-pulse experiment the observed full width at half-maximum was 0.115 V—slightly wider than the theoretical value of 0.91 V expected for a reversible process.

The potential of the couple $\text{Ru}(\text{NH}_3)_5\text{py}^{3+/2+}$ by cyclic voltammetry was +0.06 and +0.059 V on gold and glassy carbon, respectively, and 0.067 by differential-pulse polarography. The average of +0.061 V is in excellent agreement with the value of +0.063 reported by Lim et al.¹⁹

Spectrophotometric Experiments. The spectra of the ion pairs were obtained with either 5- or 10-cm path length cells.

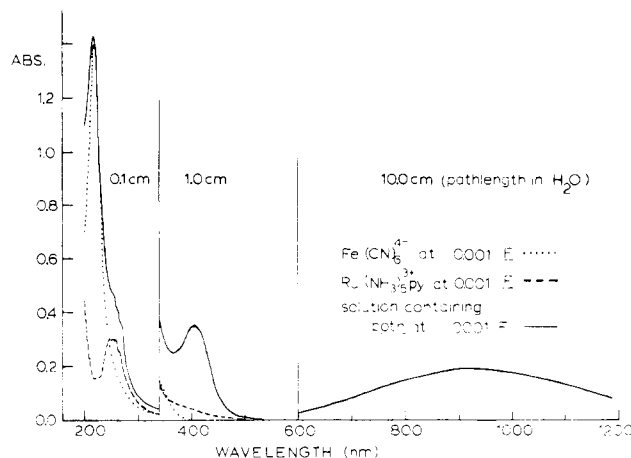


Figure 1. Spectrum of the ion pair $[\text{Fe}^{\text{II}}(\text{CN})_6, (\text{NH}_3)_5\text{Ru}^{\text{III}}\text{py}]^-$ showing the UV-vis-near-IR regions (medium: 0.09 M NaTFA, pH 5, 0.01 M HOAc/NaOAc buffer).

The procedure used was to dissolve the cationic component $[(\text{NH}_3)_5\text{Ru}^{\text{III}}(\text{L})\text{Cl}_3]$ in 5 mL of electrolyte and then rapidly mix this with an appropriate volume of a solution of the hexacyanide complex containing an equal number of equivalents (the solutions were freshly prepared each time) such that the combined volume just filled the spectrophotometer cell. The absorbance maximum and λ_{max} values had to be obtained quickly after mixing (typically within 30 s) so as to avoid any error due to the slow formation of cyano-bridged species. This problem was particularly severe for the ion pairs between ferrocyanide and the more oxidizing $[(\text{NH}_3)_5\text{Ru}^{\text{III}}(\text{L})]\text{Cl}_3$ complexes such as $\text{L} = 4\text{-Br(py)}$. It was found that for most of the ion pairs involved, precipitation of the complex salt $[(\text{NH}_3)_5\text{Ru}^{\text{III}}(\text{L})]_4[\text{M}^{\text{II}}(\text{CN})_6]_3$ ensued if the equimolar concentrations were raised above about 0.006 M.

A typical spectrum is shown in Figure 1. Due to the vastly different extinction coefficients over the different spectral regions, the figure is shown as a composite of spectra obtained in various path length cells all at a concentration of 0.001 M in each ion, $[(\text{NH}_3)_5\text{Ru}^{\text{III}}\text{py}]^{3+} = [\text{Fe}^{\text{II}}(\text{CN})_6]^{4-}$. The spectral data for all of the ion pairs investigated are summarized in Table IV.

Extinction coefficients for the low-energy outer-sphere charge-transfer (OSCT) bands were determined from the slopes of Beer's law plots in the concentration region where ion pairing was essentially 100% complete. A typical plot is shown in Figure 2. As can be seen from the figure, the linear region begins at a concentration of about 0.002 M in each ion. The spectral data for the OSCT band in the various ion pairs investigated in this study are summarized in Table IV.

Formation Constants. Once the extinction coefficient for a given ion pair was known, it became possible to analyze spectrophotometrically for the ion-pair concentration in the region of less than 100% ion pair formation.

If the ion-pair formation constant is defined as

$$K_A = \frac{[\text{ion pair}]}{[(\text{cation})-(\text{ion pair})][(\text{anion})-(\text{ion pair})]} = \frac{[\text{IP}]}{[\text{Ru}^{\text{III}}-\text{IP}][\text{M}^{\text{II}}-\text{IP}]}$$

noting that in all cases $[(\text{NH}_3)_5\text{Ru}^{\text{III}}(\text{L})]^{3+} = [\text{M}^{\text{II}}(\text{CN})_6]^{4-}$, gives

$$K_A = \{[\text{Ru}^{\text{III}}]^2 / [\text{IP}] - 2[\text{Ru}^{\text{III}}] + [\text{IP}]\}^{-1}$$

The data for the series of ion pairs $[(\text{NH}_3)_5\text{Ru}^{\text{III}}\text{py}, \text{M}^{\text{II}}(\text{CN})_6]^-$, where $\text{M} = \text{Fe}, \text{Ru}, \text{Os}$, are summarized in Table V.

(17) Kolthoff, I. M.; Tomsich, W. J. *J. Phys. Chem.* **1935**, *39*, 945.

(18) "Handbook of Chemistry and Physics", 60th ed.; CRC Press: Cleveland, OH, 1979–1980.

(19) Lim, H. S.; Barclay, D. J.; Anson, F. C. *Inorg. Chem.* **1972**, *11*, 1460.

Table III. Reduction Potentials (V vs. SCE) for the Various Complexes Employed in the Spectrophotometric Studies^a

compd	$E_{1/2}$ (gold) ^b	$E_{1/2}$ ^c (glassy carbon)	$E_{1/2}$ ^c (glassy carbon)	$E_{1/2}$ (av)
$K_4[Fe(CN)_6]$	+0.181	+0.195	+0.185	+0.187 ± 0.010
$K_4[Os(CN)_6]$	+0.382	+0.404	+0.398	+0.395 ± 0.010
$K_4[Ru(CN)_6]$		+0.699	+0.703	+0.701 ± 0.010
$[Ru(NH_3)_6]Cl_3$	-0.183			-0.183 ± 0.008
$[NH_3)_5Ru(Im)]Cl_3$	-0.140	-0.142	-0.139	-0.140 ± 0.008
$[NH_3)_5Ru(Me_2pzi)]Cl_3$	-0.085	-0.084		-0.084 ± 0.008
$[NH_3)_5Ru(pzi)]Cl_3$	-0.039	-0.047		-0.043 ± 0.008
$[NH_3)_5Ru(4-Mepy)]Cl_3$	+0.023	+0.021		+0.022 ± 0.008
$[NH_3)_5Ru(4-t-Bupy)]Cl_3$	+0.029	+0.033		+0.030 ± 0.008
$[NH_3)_5Ru(py)]Cl_3$	+0.060	+0.059	+0.067	+0.062 ± 0.008
$[NH_3)_5Ru(4-Cl(py))Cl_3$	+0.100	+0.095		+0.097 ± 0.008
$[NH_3)_5Ru(4-Br(py))Cl_3$	+0.102	+0.096		+0.100 ± 0.008
$[NH_3)_5Ru(3-Cl(py))Cl_3$	+0.126	+0.123		+0.124 ± 0.008
$[NH_3)_5Ru(3,5-Cl_2py)Cl_3$	+0.186	+0.188		+0.187 ± 0.008
$[NH_3)_5Ru(Me_2pyz)]Cl_3$	+0.226	+0.229	+0.229	+0.227 ± 0.008

^a All measurements performed in a medium of 0.09 M NaTlFA and a 0.01 M NaOAc/HOAc buffer. ^b $E_{1/2}$ values as determined from cyclic voltammograms at 200 mV/s sweep rate. ^c $E_{1/2}$ values as determined from differential-pulse polarograms at 5-mV modulation amplitude and 1 mV/s scan rate.

Table IV. Spectral and Thermodynamic Data for the OSCT Bands in the Various Ion Pairs Studied^a

M	$(NH_3)_5Ru^{III}(L)^{3+}$	λ_{max}	$10^{-3}\epsilon_{max}^b$	$\Delta H_{ip}^{c,e}$	ϵ_{max}^b	$10^{-3}\Delta\nu_{1/2}$ (direct), ^d	$10^{-3} \times \Delta\nu_{1/2}$ (doubling), ^e	$\Delta\nu_{1/2}$ (doubling)/ $\Delta\nu_{1/2}$ (direct)	$\Delta\nu_{1/2}$ (theor) ^f	$10^6 \alpha^2 g$	β, h cm ⁻¹
Fe	4-Br(py)	932 ± 15	10.72 ± 0.2	15.63 ± 0.8	29 ± 5	6.1 ± 0.3	4.6 ± 0.1	1.33	3.7	1.6	108
Fe	4-Cl(py)	940 ± 15	10.64 ± 0.2	15.70 ± 0.8	32 ± 5	(6.6)	5.7 ± 0.1		3.7	1.8	118
Fe	py	910 ± 15	10.99 ± 0.2	16.50 ± 0.8	33 ± 3	6.3 ± 0.3	5.9 ± 0.1	1.10	3.7	1.7	119
Fe	4-Mepy	898 ± 15	11.14 ± 0.2	17.42 ± 0.8	33 ± 5	6.3 ± 0.3	5.3 ± 0.1	1.19	3.7	1.7	119
Fe	4-t-Bupy	894 ± 20	11.18 ± 0.3	17.23 ± 0.8	30 ± 5	6.1 ± 0.3	5.9 ± 0.1	1.03	3.7	1.7	112
Fe	pzi	864 ± 10	11.84 ± 0.2	18.92 ± 0.8	36 ± 5	(6.6)	5.8 ± 0.1		3.7	1.8	125
Fe	Im	810 ± 20	12.35 ± 0.3	19.87 ± 0.8	29 ± 5	(7.1)	6.1 ± 0.1		3.7	1.9	125
Ru	Me ₂ pyz	788 ± 8	12.69 ± 0.1	21.19 ± 0.8	28 ± 5	(6.5)	5.6 ± 0.1		3.7	1.7	119
Ru	3,5-Cl ₂ (py)	700 ± 10	14.29 ± 0.2	24.55 ± 0.8	39 ± 5	(7.7)	6.5 ± 0.1		3.9	2.0	159
Ru	3-Cl(py)	675 ± 10	14.81 ± 0.2	25.48 ± 0.8	31 ± 5	(7.8)	6.6 ± 0.1		3.9	2.0	145
Ru	4-Br(py)	665 ± 10	15.19 ± 0.2	26.93 ± 0.8	37 ± 5	7.3 ± 0.3	6.1 ± 0.1	1.20	3.9	1.9	155
Ru	4-Cl(py)	653 ± 10	15.31 ± 0.2	27.48 ± 0.8	35 ± 5	8.2 ± 0.3	6.9 ± 0.1	1.19	3.9	2.1	161
Ru	py	656 ± 10	15.23 ± 0.2	27.55 ± 0.8	36 ± 5	7.4 ± 0.3	6.4 ± 0.1	1.16	3.9	1.9	154
Ru	4-Mepy	643 ± 10	15.55 ± 0.2	28.36 ± 0.8	38 ± 3	8.1 ± 0.3	6.1 ± 0.1	1.18	3.9	1.8	157
Ru	Os	627 ± 10	15.95 ± 0.2	29.28 ± 0.8	38 ± 5	9.1 ± 0.4	8.3 ± 0.1	1.21	3.9	2.1	170
Os	Os	716 ± 10	13.97 ± 0.2	17.50 ± 0.8	30 ± 8	(9.0)	8.4 ± 0.1	1.10	4.4	2.0	181
Os	3,5-Cl ₂ (py)	700 ± 10	14.28 ± 0.2	18.42 ± 0.8	44 ± 5	8.6 ± 0.3	7.7 ± 0.1	1.11	4.4	1.9	178
Os	4-Br(py)	670 ± 10	14.93 ± 0.2	20.43 ± 0.8	42 ± 5	9.7 ± 0.3	8.5 ± 0.1	1.14	4.5	2.1	187
Os	3-Cl(py)	668 ± 10	14.97 ± 0.2	19.86 ± 0.8	41 ± 5	(9.0)	8.2 ± 0.1		4.4	2.0	181
Os	py	658 ± 8	15.29 ± 0.2	21.30 ± 0.8	40 ± 5	9.3 ± 0.5	9.0 ± 0.1	1.03	4.6	2.0	198
Os	4-t-Bupy	625 ± 15	16.00 ± 0.3	22.04 ± 0.8	45 ± 8	8.9 ± 0.3	8.3 ± 0.1	1.08	4.5	2.0	180
Os	4-Mepy	626 ± 10	15.97 ± 0.2	22.23 ± 0.8	39 ± 5						

^a All spectra obtained at 23 ± 2 °C in the electrolytic mixture of 0.09 M NaTlFA and a 0.01 M NaOAc/NgOAc pH 5 buffer. ^b Error limits estimated on the basis of the reproducibility of the data (all considerably exceeding instrumental limits). ^c Calculated from eq 13. ^d Bandwidth at half-maximum from direct measurement. ^e Values in parentheses are estimated by multiplying the $\Delta\nu$ (doubling) value by the average ratio of $\Delta\nu$ (direct)/ $\Delta\nu$ (doubling) obtained from those points where both were measurable. ^f Bandwidth at half-maximum obtained by simply doubling the width obtained from the low-energy side of the band. ^g Calculated from eq 14. ^h Calculated from eq 20.

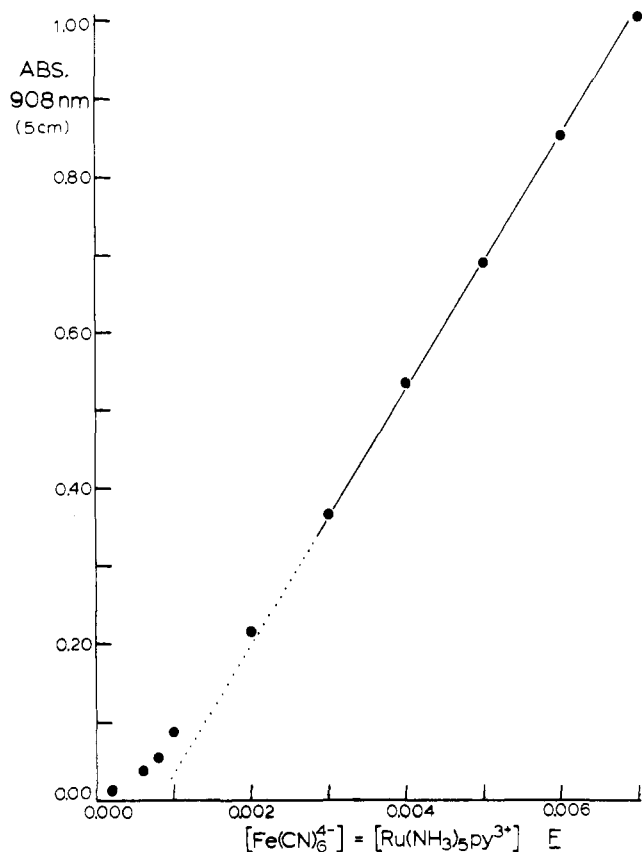


Figure 2. Beer's law plot for the ion pair $[\text{Fe}^{\text{II}}(\text{CN})_6, (\text{NH}_3)_5\text{Ru}^{\text{III}}\text{py}]^-$ at $23 \pm 2^\circ\text{C}$ in a medium of $0.09\text{ M Na}^+\text{CF}_3\text{CO}_2^-$ and $0.01\text{ M pH } 5\text{ NaOAc/HOAc}$ buffer.

From Table V it is seen that the formation constants for the ion pairs $[\text{M}^{\text{II}}(\text{CN})_6, \text{Ru}^{\text{III}}(\text{NH}_3)_5\text{py}]^-$ are all equal within experimental error. This is to be expected on the basis of the form of the Eigen-Fuoss equation for ion pair association²⁰

$$K_{12}^A = \frac{4\pi N_0 d^3}{3000} \exp\left(\frac{-Z_1 Z_2 e_0^2}{d D_s (1 + \kappa d) RT}\right) \quad (2)$$

$$\kappa = \left[\frac{8\pi^2 e_0^2 \mu}{1000 D_s RT} \right]^{1/2}$$

where d is the interreactant separation, D_s is the static dielectric constant, Z_1 and Z_2 are the charges on the reactants, e_0 is the unit electronic charge, and μ is the ionic strength. Clearly, for a series of ion pairs in which the charge types and separation distances are constant, eq 2 predicts equal association constants (a discussion of the evaluation of the distances involved is presented later).

The value of $(2.5 \pm 0.3) \times 10^3\text{ M}^{-1}$ obtained for the iron system is in very good agreement with the value $2.4 \times 10^3\text{ M}^{-1}$ derived kinetically by Miralles et al. for the ion pair $[\text{Fe}^{\text{II}}(\text{CN})_6, \text{Co}^{\text{III}}(\text{NH}_3)_5\text{py}]^-$.²¹ Again, this would be predicted from eq 2 on the basis of the similarities in the sizes and charge types involved in the two different association processes.

The analysis presented here is based on the assumption that the ion pairs formed are of a 1:1 formulation. Formation of 2:1 pairs such as $[(\text{NH}_3)_5\text{Ru}^{\text{III}}\text{py}, \text{Ru}^{\text{II}}(\text{CN})_6]^-$, $[(\text{NH}_3)_5\text{Ru}^{\text{III}}\text{py}]^{3+}$ can be shown to be considerably less favorable via eq 2 (the theoretically predicted formation constant drops from 4.5×10^2 to 10). However, experimental evidence

Table V. Ion-Pair Formation Data for the Ion Pairs $[(\text{NH}_3)_5\text{Ru}^{\text{III}}\text{py}, \text{M}^{\text{II}}(\text{CN})_6]^-$, Where $\text{M} = \text{Fe}, \text{Ru}, \text{Os}^a$

$10^4 \times$ $[(\text{NH}_3)_5\text{Ru}^{\text{III}}\text{py}]^{3+} =$ $[\text{Fe}^{\text{II}}(\text{CN})_6]^{4-}, \text{M}$	abs at 910 nm^b	$10^4 \times$ [ion pair], $\text{M} (\epsilon 33 \pm 5$ $\text{M}^{-1} \text{cm}^{-1})$	% ion pairing	$10^{-3} K^A,$ M^{-1}
1.00	0.0068	0.206	21	3.3
2.00	0.0166	0.503	25	2.2
2.90	0.0288	0.873	30	2.6
4.83	0.0588	1.782	37	1.9
				av = 2.5 ± 0.3
$10^4 \times$ $[(\text{NH}_3)_5\text{Ru}^{\text{III}}\text{py}]^{3+} =$ $[\text{Ru}^{\text{II}}(\text{CN})_6]^{4-}, \text{M}$	abs at 643 nm^b	$10^4 \times$ [ion pair], $\text{M} (\epsilon 38$ $\text{M}^{-1} \text{cm}^{-1})$	% ion pairing	$10^{-3} K^A,$ M^{-1}
1.00	0.0088	0.232	23	3.9
2.00	0.0210	0.553	28	2.6
3.00	0.0371	0.976	33	2.4
4.00	0.0573	1.510	38	2.4
5.00	0.0813	2.140	43	2.6
				av = 2.7 ± 0.3
$10^4 \times$ $[(\text{NH}_3)_5\text{Ru}^{\text{III}}\text{py}]^{3+} =$ $[\text{Os}^{\text{II}}(\text{CN})_6]^{4-}, \text{M}$	abs at 656 nm^b	$10^4 \times$ [ion pair], $\text{M} (\epsilon 40$ $\text{M}^{-1} \text{cm}^{-1})$	% ion pairing	$10^{-3} K^A,$ M^{-1}
1.00	0.0082	0.230	23	3.9
2.00	0.0171	0.427	21	2.0
3.00	0.0437	1.093	36	4.1
4.00	0.0564	1.413	46	2.7
5.00	0.064	1.60	32	1.8
				av = 2.9 ± 0.6

^a All at $23 \pm 2^\circ\text{C}$ in a medium of 0.09 M NaTFA and a $0.10\text{ M pH } 5\text{ NaOAc/HOAc}$ buffer. ^b In 10-cm path length cells.

for 2:1 ion pair formation is observed in solutions where one species is in large excess over the other. For example, in a solution of $0.001\text{ M K}_4[\text{Ru}^{\text{II}}(\text{CN})_6]$, $\lambda_{\text{max}} = 643 \pm 8\text{ nm}$ when $[(\text{NH}_3)_5\text{Ru}^{\text{III}}\text{py}]^{3+} = 0.001\text{ M}$ but blue shifts somewhat to $\lambda_{\text{max}} = 630\text{ nm}$ when $[(\text{NH}_3)_5\text{Ru}^{\text{III}}\text{py}]^{3+} = 0.032\text{ M}$.

In Table IV it is seen that in general the extinction coefficients of the OSCT bands of the osminocyanide ion pairs are slightly higher than those of the ruthenocyanide ion pairs, which, in turn, are higher than those of ferrocyanide. Also, it is seen that, in general, the band width at half-maximum increases significantly upon going from iron to ruthenium to osmium.

By comparison of the band widths at half-maximum as determined directly from the whole band (not possible in some cases) with those obtained by simply doubling the value obtained from the low-energy side, it is seen that the bands are slightly asymmetric—being skewed toward higher energy. By comparison of the ratios $\Delta\nu_{1/2}(\text{doubling})/\Delta\nu_{1/2}(\text{direct})$ obtained from the two methods it is seen that the ferrocyanide and ruthenocyanide ion pairs are asymmetric by about 15% and the osminocyanide ion pairs appear, on the average, to be slightly less asymmetric—although this judgment is quite uncertain owing to the $\pm 7\%$ compound error in the ratios.

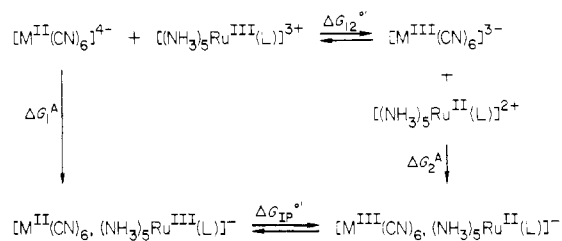
The increase in energy of the band maximum down the series of ligands L for each hexacyanide species is of relevance to the arguments presented later based on eq 3 as discussed below.

The time evolution of the OSCT spectra is a matter of some interest. In all cases, it was observed that the λ_{max} and absorbance values began to evolve significantly within 2–3 min of mixing the two components together—with λ_{max} shifting to longer wavelengths and the absorbance increasing. This was attributed to the probable formation of cyano-bridged

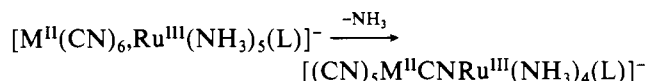
(20) (a) Fuoss, C. M. *J. Am. Chem. Soc.* **1958**, *80*, 5059. (b) Eigen, M. Z. *Phys. Chem. (Wiesbaden)* **1954**, *1*, 176.

(21) Miralles, A. J.; Armstrong, R. E.; Haim, A. *J. Am. Chem. Soc.* **1977**, *99*, 1416.

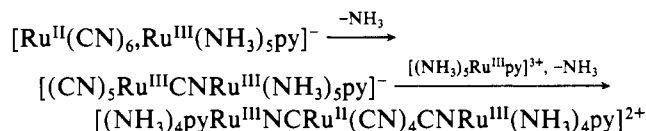
Scheme I



species which would be expected to have IT bands of both lower energy and higher intensity than the outer-sphere ion pairs.



Upon closer investigation of the spectra of the ion pair $[\text{Ru}^{II}(\text{CN})_6, \text{Ru}^{III}(\text{NH}_3)_5\text{py}]^{-}$, it was found that λ_{max} increased from an initial value of 643 to a maximum of about 780 nm in 10 h followed by a steady increase in the absorbance (with no further shift in λ_{max}) over a period of several days. Subsequent exposure to room light caused a rather rapid shift (over a period of 6–8 h) to a λ_{max} of ~ 700 nm. This behavior was observed for a solution that was initially 0.002 M in each component. More concentrated solutions evolved more rapidly. This sequence is taken as suggestive of dimer formation followed by trimer formation.



Apparently, the first step occurs thermally while the second step is initiated photochemically.

The dimer is expected to absorb at lower energy and with greater intensity than the ion pair due to the shorter distance between the redox sites and the resulting greater degree of electronic interaction.²² The trimeric species is expected to absorb at slightly higher energy than the dimer simply on the basis of electronic effects; a ruthenocyanide flanked by two ruthenium(III) pentaammine sites should be somewhat harder to oxidize than a dimer in which there is a single pentaammine site.

In support of this suggestion is the fact that the dimeric system $\text{Li}[\text{trans}-[(\text{CN})_5\text{Ru}^{II}\text{CNRu}^{III}(\text{NH}_3)_4\text{py}]]$ prepared as described in the Experimental Section has its λ_{max} at 780 nm with an extinction coefficient of $7.7 \times 10^3 \text{ M}^{-1} \text{ cm}^{-1}$. In the differential-pulse polarogram of this ion are two peaks of approximately equal areas. In the dimer the ruthenocyanide couple is shifted anodically to +0.93 V from the +0.703 V potential of the free monomeric ion. The rutheniumammine couple is cathodically shifted to a value of -0.04 V as compared to the free complex value of +0.062 V. This indicates a substantial degree of electron donation from the ruthenocyanide complex to the ammineruthenium center in the dimeric system. Support for the assignment of the final species as the trimer comes from the fact that the dark blue cationic material which washes straight through an anion-exchange resin and which results from the reaction between $[\text{trans}-\text{SO}_4\text{Ru}^{III}(\text{NH}_3)_5\text{py}]^{+}$ and ruthenocyanide exhibits a λ_{max} of 717 nm.

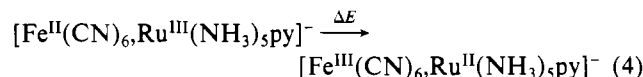
Discussion

With spectral and redox potential data in hand, we are in a position to test the application of available theory to the OSCT bands. In addition, from the properties of the bands

it will prove possible to reach some interesting conclusions concerning structure in the ion pairs, the extent of electronic interaction between outer-sphere electron donors and acceptors, and the existence of multiple OSCT bands arising from the effects of spin-orbit coupling on the d^5 core of the $\text{M}(\text{CN})_6^{3+}$ site formed in the optical charge-transfer process.

In the classical limit the energies of optical CT bands for a chemically related series of mixed-valence dimers, or as in this case, electron donor-acceptor ion pairs should vary as in eq 3.^{3,5,8} In eq 4, ΔE is the internal energy difference between

$$E_{\text{op}} = \chi + \Delta E \quad (3)$$



the different oxidation state distributions within the ion pair. The term χ_i , or rather $\chi/4$, is the classical vibrational trapping energy which has contributions from two sources, intramolecular vibrations (χ_i) and low-frequency, collective vibrations of the surrounding medium (χ_o) (eq 5). The relatively simple

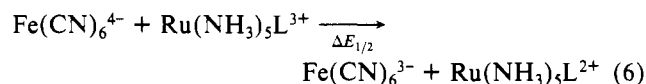
$$\chi = \chi_i + \chi_o \quad (5)$$

form of eq 3 relies on certain assumptions including the use of harmonic oscillator vibrational potential functions and equal vibrational force constants before and after charge transfer.

E_{op} is simply the band maximum for an OSCT absorption band. ΔE can be obtained or at least estimated from formal potentials, obtained from $E_{1/2}$ measurements, for the redox couples involved. However, before proceeding further, the thermodynamics of charge transfer within the ion pairs must be considered in some detail.

Thermodynamics of Charge Transfer within the Ion Pairs.

The redox potential values in Table III allow calculation of $\Delta E_{1/2}$ which is basically the free energy change for electron transfer between the separated ions in the appropriate medium. The quantity needed to test eq 3 is the internal energy change upon charge transfer within the ion pair (eq 4) or since $\Delta E \approx \Delta H_{\text{IP}}^{\circ}$, the corresponding enthalpy difference.



The free energy change for eq 6 is given by the equation below in terms of the redox potentials of the individual couples.

$$\Delta G^{\circ} = -nF(E_{1/2}[(\text{NH}_3)_5\text{Ru}^{III/II}\text{L}] - E_{1/2}[\text{M}^{III/II}(\text{CN})_6]) = -nF\Delta E_{1/2}$$

In order for the thermodynamic free energy change germane to electron transfer within the ion pair itself, $\Delta G_{\text{IP}}^{\circ}$, to be evaluated, the cycle in Scheme I must be considered, from which $\Delta G_{\text{IP}}^{\circ}$ is given by eq 7.²³

$$\Delta G_{\text{IP}}^{\circ} = \Delta G_{12}^{\circ} - \Delta G_1^A + \Delta G_2^A \quad (7)$$

The free energies of association, ΔG_1^A , for the ion pairs $[\text{M}^{II}(\text{CN})_6, (\text{NH}_3)_5\text{Ru}^{III}\text{py}]^{-}$, where $\text{M} = \text{Fe}, \text{Ru}, \text{Os}$, are calculated to be -4.60 ± 0.07 , -4.65 ± 0.07 , -4.65 ± 0.07 , and -4.69 ± 0.14 kcal/mol, respectively, from the equilibrium constants reported in Table V. Unfortunately, the values for the opposite leg of the cycle, ΔG_2^A , cannot be evaluated directly. However, theoretical estimate for this quantity is available from eq 2 but written as a free energy (eq 8) change where the symbols are defined as previously.

(23) It should be noted that eq 7 does not appear to take into account in a specific way variations in electronic coupling between the donor and acceptor redox sites which, for example, play an important role in the Mulliken theoretical approach to donor-acceptor complexes. However, as discussed below, electron coupling is relatively weak (~ 100 – 200 cm^{-1}) and variations are small. It should also be noted that electronic coupling effects are included in the measured values of ΔG_1^A and ΔG_2^A .

$\Delta G^A(\text{Eigen-Fuoss}) =$

$$\frac{Z_1 Z_2 e_0^2}{D_s d} \frac{1}{1 + \kappa d} - RT \ln \left(\frac{4\pi N_0 d^3}{3000} \right) \quad (8)$$

The hard-sphere interreactant distance d is calculated as being 8.3 Å in the case of the $[\text{Fe}^{\text{II}}(\text{CN})_6, (\text{NH}_3)_5\text{Ru}^{\text{III}}\text{py}]^-$ ion pair and 8.5 Å for the rutheno- and osminocyanide ion pairs. The model adopted here assumes that the ion pairs form at the van der Waals contact between the hexacyanide moiety and the ammine face of the ruthenium(III) complex (evidence for the validity of this hypothesis will be discussed later). The distances are calculated on the basis of the crystallographic data of Creutz,⁴ Swanson,²⁴ Ibers,²⁵ Ludi²⁶ and the known van der Waals radii of hydrogen and nitrogen.²⁷ Strictly speaking, the second term in eq 8 is a consequence of a volume exclusion, so the radius of the ammineruthenium(III) complex used in calculating this distance should be the radius of a sphere of equal volume rather than simply the distance over which the Coulombic interaction takes place. Thus, $\bar{r} = 1/2(D_1 D_2 D_3)^{1/3}$, where D_1 , D_2 , and D_3 are the lengths of the three different L-Ru-L axes.²⁸ In the case considered here, the three lengths are identical at 7.6 Å ($\text{H}_3\text{N-Ru}^{\text{III}}-\text{NH}_3$) while the third is 10.8 Å ($\text{py-Ru}^{\text{III}}-\text{NH}_3$) which gives $\bar{r} = 4.3$ Å. With this value for \bar{r} , d in eq 8 is 8.9 Å for the ferrocyanide ion pair and 9.0 Å for the rutheno- and osminocyanide ion pairs (in the absence of structural information, the osminocyanide dimensions have been taken as being equal to those of the ruthenocyanide complex).

With use of eq 8 for the ion pair $[\text{Fe}^{\text{II}}(\text{CN})_6, (\text{NH}_3)_5\text{Ru}^{\text{III}}\text{py}]^-$, $\Delta G_1^A = -3.6$ kcal/mol, which is in only fair agreement with the experimental value of -4.91 ± 0.08 kcal/mol.

As discussed in an earlier paper on a related system, we have used eq 9 to calculate ΔG_2^A .²⁹ With eq 9, the following values

$$\Delta G_2^A = \Delta G_2^A(\text{Eigen-Fuoss}) \frac{\Delta G_1^A(\text{exptl})}{\Delta G_1^A(\text{Eigen-Fuoss})} \quad (9)$$

were obtained: $\Delta G_2^A([\text{Fe}^{\text{III}}(\text{CN})_6, (\text{NH}_3)_5\text{Ru}^{\text{II}}\text{py}]^-) = -2.67 \pm 0.04$ kcal/mol, $\Delta G_2^A([\text{Ru}^{\text{III}}(\text{CN})_6, (\text{NH}_3)_5\text{Ru}^{\text{II}}\text{py}]^-) = -2.56 \pm 0.04$ kcal/mol, and $\Delta G_2^A([\text{Os}^{\text{III}}(\text{CN})_6, (\text{NH}_3)_5\text{Ru}^{\text{II}}\text{py}]^-) = -2.58 \pm 0.08$ kcal/mol.

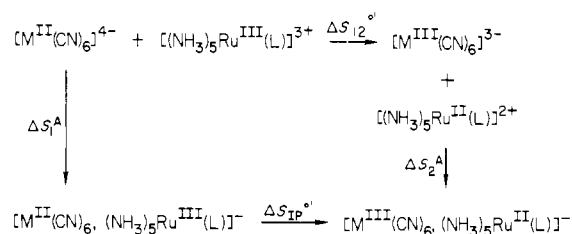
From the values of G_1^A and G_2^A the effect of ion pairing is to increase the redox asymmetry in the ion pairs by 2.1 ± 0.1 kcal/mol (0.091 ± 0.004 V) compared to the free ions. The numerical values are related to each other by eq 10, which follows from eq 7.

$$\Delta G_{\text{IP}}^{\circ'} = \Delta G_{12}^{\circ'} + 2.1 \pm 0.1 \text{ kcal/mol} \quad (10)$$

The discrepancy between the experimentally observed value for ΔG_1^A ($\Delta G_1^A(\text{exptl})/\Delta G_1^A(\text{Eigen-Fuoss}) \simeq 1.4$) and the theoretical value calculated from eq 8 probably reflects in part the fact that there is a strong, favorable hydrogen-bonding interaction in the ion pair that is not included in the Eigen-Fuoss treatment. The existence of hydrogen-bonding interactions in similar systems has been demonstrated via infrared spectroscopy by Casabo and Ribas.³⁰

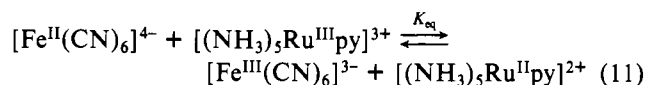
In considering the extended series of ion pairs based on the $[(\text{NH}_3)_5\text{Ru}^{\text{III}}(\text{L})]^{3+}$ complexes, variations in the effective distance d are insignificant numerically and the simple am-

Scheme II



mine-face contact distance could be used for them all without significant loss in accuracy.

A cycle (Scheme II) analogous to that in Scheme I can be used to calculate $\Delta S_{\text{IP}}^{\circ'}$, the entropy change associated with electron transfer within the ion pair. A value of $\Delta S^{\circ'} = +46 \pm 6$ eu has been measured by Miralles et. al²¹ for the reaction in eq 11. As noted by these workers, such a large, positive



entropy change is expected for a reaction in which net charge neutralization occurs because of the lesser degree of electrostriction of the solvent molecules surrounding the reactant ions following electron transfer.

The entropy of association for the ion pair of the reactants, ΔS_1^A , was also measured by Miralles et. al but for the ion pair between pentaammine(pyridine) cobalt(III) and ferrocyanide. Since $[(\text{NH}_3)_5\text{Co}^{\text{III}}\text{py}]^{3+}$ and $[(\text{NH}_3)_5\text{Ru}^{\text{III}}\text{py}]^{3+}$ are of similar size and identical charge type, it will be assumed here that the value ΔS_1^A for the association between $[\text{Fe}^{\text{II}}(\text{CN})_6]^{4-}$ and $[(\text{NH}_3)_5\text{Ru}^{\text{III}}\text{py}]^{3+}$ is the same as the value of $+15 \pm 5$ eu reported for the cobalt system (no error limits were reported with this number; the ± 5 is our own estimate). The assumption of a metal ion independent value of ΔS_1^A is strongly supported by the fact that the measured values of ΔG_1^A for the association of $[\text{M}(\text{NH}_3)_5\text{py}]^{3+}$ ($\text{M} = \text{Co}, \text{Ru}$) with ferrocyanide are identical within experimental error ($\Delta G_1^A[\text{Fe}^{\text{II}}(\text{CN})_6, (\text{NH}_3)_5\text{Co}^{\text{III}}\text{py}]^- = -RT \ln 2.4 \times 10^3 = -4.58$ kcal/mol).²¹

For the ΔS_2^A leg of the cycle, a theoretical estimate is again necessary, and from the Eigen-Fuoss models ΔS_1^A is given by eq 12 where $\theta = -\partial \ln D_s / \partial \ln T = 1.368$ for water at 25

$$\Delta S^A(\text{Eigen-Fuoss}) = \frac{-Z_1 Z_2 e_0^2}{D_s d T} \frac{2\theta + \theta \kappa d + \kappa d}{2(1 + \kappa d)^2} + R \ln \left(\frac{4\pi N_0 d^3}{3000} \right) \quad (12)$$

$^{\circ}\text{C}$.²⁸ From eq 12 $\Delta S^A = +15.3$ eu for the ion pair between $[\text{Fe}^{\text{III}}(\text{CN})_6]^{4-}$ and $[(\text{NH}_3)_5\text{Ru}^{\text{III}}\text{py}]^{3+}$, which is in excellent agreement with the experimental value of $+15 \pm 5$ eu. For ΔS_2^A , eq 12 gives $+8.2$ eu, thus from the entropic analogue of eq 8

$$\Delta S_{\text{IP}}^{\circ'} = \Delta S_{12}^{\circ'} - \Delta S_1^A + \Delta S_2^A = +39 \pm 6 \text{ eu}$$

and it will be assumed that this value applies within its estimated error limits to all of the ion pairs of concern here.

With $\Delta G_{\text{IP}}^{\circ'}$ and $\Delta S_{\text{IP}}^{\circ'}$ known, the enthalpy change upon electron transfer within the ion pairs can be calculated from eq 13. The values of $\Delta H_{\text{IP}}^{\circ'}$ calculated for the various ion pairs are listed in Table IV along with the spectroscopic data for the OSCT bands.

$$\Delta H_{\text{IP}}^{\circ'} = \Delta G_{\text{IP}}^{\circ'} + T \Delta S_{\text{IP}}^{\circ'} \quad (13)$$

Relationship between the Spectroscopic and Thermodynamic Data. Figure 3 shows the plots of E_{op} (kcal/mol) vs. $\Delta H_{\text{IP}}^{\circ'}$ (kcal/mol) obtained for the ion pairs derived from the three different series based on $\text{Ru}(\text{NH}_3)_5(\text{L})^{3+}$ and $\text{M}(\text{CN})_6^{4-}$ (M

(24) (a) Swanson, B.; Jones, L. *Inorg. Chem.* **1974**, *13*, 313. (b) Swanson, B.; Rafalko, J. *Ibid.* **1976**, *15*, 249.

(25) Stynes, H. C.; Ibers, J. A. *Inorg. Chem.* **1971**, *10*, 2304.

(26) Ruegg, M.; Ludi, A.; Rieder, K. *Inorg. Chem.* **1971**, *10*, 1773.

(27) Reference 18, p F-217, D-149.

(28) Brown, G. M.; Sutin, N. *J. Am. Chem. Soc.* **1979**, *101*, 883.

(29) Curtis, J. C.; Sullivan, B. P.; Meyer, T. *J. Inorg. Chem.* **1980**, *19*, 3833-3839.

(30) Casabo, J.; Ribas, J. *Inorg. Chim. Acta* **1977**, *21*, 5.

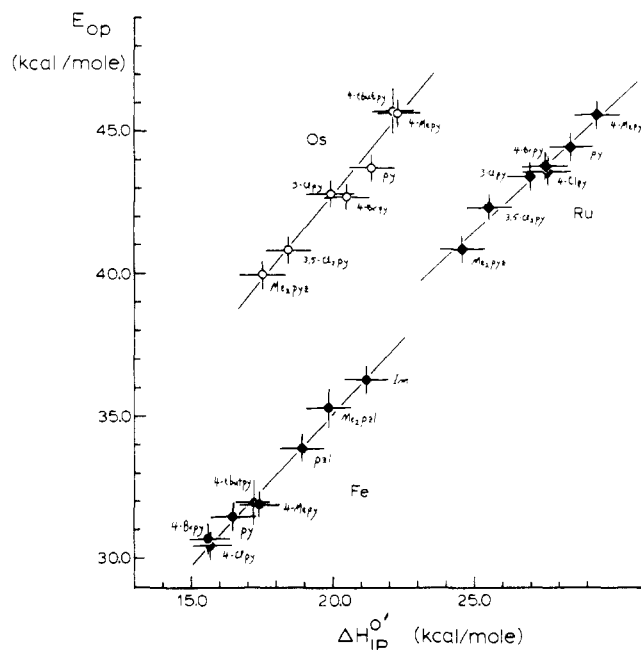
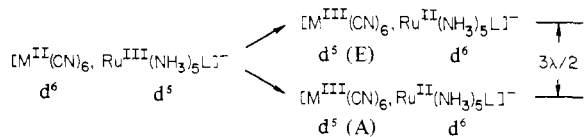


Figure 3. E_{op} vs. H_{IP}^o for the three series of ion pairs $[M^{II}(\text{CN})_6(\text{NH}_3)_5\text{Ru}^{III}(\text{L})]^-$ ($M = \text{Fe}, \text{Ru}, \text{Os}$). L is a pyridine derivative as shown in Table I.

= Fe, Ru, Os). In all cases the linear relationship between E_{op} and ΔH_{IP}^o predicted by eq 3 holds very well. The slopes of the lines, 1.08 ± 0.17 for $[\text{Fe}^{II}(\text{CN})_6\text{Ru}^{III}(\text{NH}_3)_5(\text{L})]^-$, 1.23 ± 0.33 for $[\text{Os}^{II}(\text{CN})_6\text{Ru}^{III}(\text{NH}_3)_5(\text{L})]^-$, and 0.94 ± 0.26 for $[\text{Ru}^{II}(\text{CN})_6\text{Ru}^{III}(\text{NH}_3)_5(\text{L})]^-$, are all within experimental error of the theoretical slope 1. The error limits on the slopes were computed from the results of both X - and Y -weighted linear regressions, and, as can be seen from the results, they are of sufficient magnitude that neither the observed differences in the slopes between series nor the difference between the slopes and 1 can be confidently deemed significant.

The intercepts obtained from the plots in Figure 3 increase in the order $\text{Fe} < \text{Ru} < \text{Os}$ with the values being 13.5 ± 2 , 18.4 ± 4 , and 18.6 ± 5 kcal/mol, respectively. Since, from eq 3, these intercepts are the sums of χ_{inner} and χ_{outer} , it is not unreasonable that they would vary from one series to the other. Although, as discussed below, χ_o might be expected to remain reasonably constant throughout the series, χ_i could well vary significantly with the nature of the $\text{M}(\text{CN})_6^{4-}$ ion.

However, there is an additional factor, electronic in nature, that must be considered in analyzing the OSCT bands. In the O_h symmetry of the hexacyano ions, the effect of spin-orbit coupling is to split the d^5 core into two states: a degenerate E state and a nondegenerate A state $3\lambda/2$ lower in energy.³⁰ λ is the spin-orbit coupling constant. For an OSCT band, there should be two contributing transitions:



In the simplest model, where ion pairing does not perturb the degeneracy of the E set, there should be two components: a low-energy band and a band twice as intense $3\lambda/2$ higher in energy.

Evidence for the importance of spin-orbit components in the OSCT bands comes from comparisons between experimental band widths and widths calculated theoretically from eq 14.³ Equation 14 is based on the assumption of harmonic

$$\Delta\bar{\nu}_{1/2}(\text{theor}) = [2.3 \times 10^3(E_{op} - E)]^{1/2} \quad (14)$$

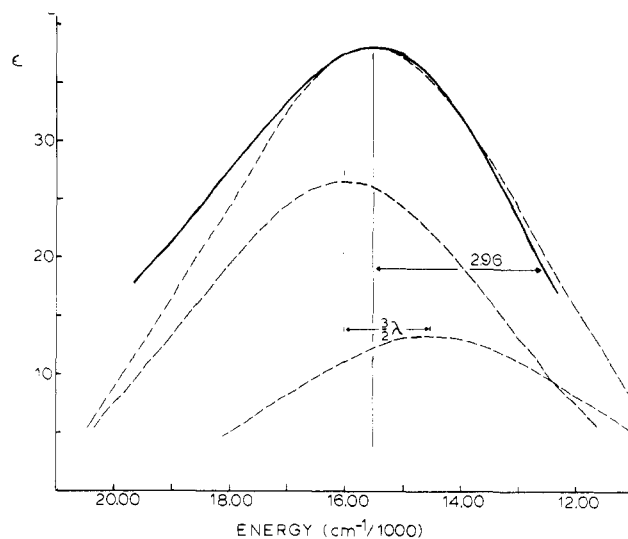


Figure 4. The OSCT band for the ion pair $[\text{Ru}^{II}(\text{CN})_6(\text{NH}_3)_5\text{Ru}^{III}\text{py}]^-$ plotted vs. energy and fit by two spin-orbit components. $\lambda = 1000 \text{ cm}^{-1}$.

oscillator potential functions. Because of anharmonicity and other effects, $\Delta\bar{\nu}_{1/2}(\text{obsd})/\Delta\bar{\nu}_{1/2}(\text{theor})$ is expected to exceed 1 and does for a series of electronically weakly coupled mixed-valence dimers. However, the ratios of the ion pairs in Table IV are quite large especially for the Ru and Os cases. It should also be noted that well-resolved spin-orbit transitions have been observed for the mixed-valence dimer $(\text{bpy})_2\text{ClOs}^{II}(\text{Ph}_2\text{PCH}_2\text{PPh}_2)\text{Os}^{III}\text{Cl}(\text{bpy})_2^{3+,31}$

In Figure 4 is shown a plot of the OSCT band for $[\text{Ru}^{II}(\text{CN})_6(\text{NH}_3)_5\text{Ru}^{III}\text{py}]^-$ and an attempted fit of the bands with two Gaussian components at an intensity ratio of 2:1 and split by $3\lambda/2$. λ was taken to be 1000 cm^{-1} .³⁰ It is seen that the band maximum, intensity, and a significant portion of the low-energy side of each band can be fit in this manner. The width at half-height of the two components was taken as equal to the width obtained by doubling the experimental value for the low-energy side of the band in the ion pair $[\text{Fe}^{II}(\text{CN})_6(\text{NH}_3)_5\text{Ru}^{III}\text{py}]^-$. The reason for this strategy was that the high-energy sides of the bands are significantly skewed and widened as is normal for charge-transfer bands where the potential energy surfaces are significantly displaced.³ Similar agreement was obtained for the iron case using $\lambda = 410 \text{ cm}^{-1}$ ³⁰ and for $\text{Os}(\text{CN})_6^{4-}$ case using $\lambda = 2500 \text{ cm}^{-1}$.

The relationship suggested by eq 3 is only correct in considering the lowest spin-orbit state transition. For the higher energy component, it follows that $E_{op} = \lambda + \Delta E + 3\lambda/2$ ($\Delta E = \Delta H_{IP}^o$). In Figure 5 are shown plots of E_{op}' vs. ΔH_{IP}^o , where E_{op}' is the energy of the lower spin-orbit transition estimated from the spectral fitting procedure described above and illustrated in Figure 4. The effect of plotting E_{op}' is dramatic in that the plots for the three systems nearly coalesce into a single line. The intercepts obtained for the ferro-, rutheno-, and osminocyanide series are now 12.6 ± 2 , 15.5 ± 4 , and 10.1 ± 5 kcal/mol, respectively, which are all essentially within experimental and calculational error of one another. Although variations in χ_i may appear in the data, it seems clear that once corrections for spin-orbit effects are made, the energetics of the three series are closely related.

It is possible to estimate χ , which is 4 times the classical vibrational trapping energy, from available theoretical equations. The magnitude of the intramolecular vibrational contribution is given by eq 15, where $\chi_{11,i}$ and $\chi_{22,i}$ are the con-

$$\chi_i = (\chi_{11,i} + \chi_{22,i})/2 \quad (15)$$

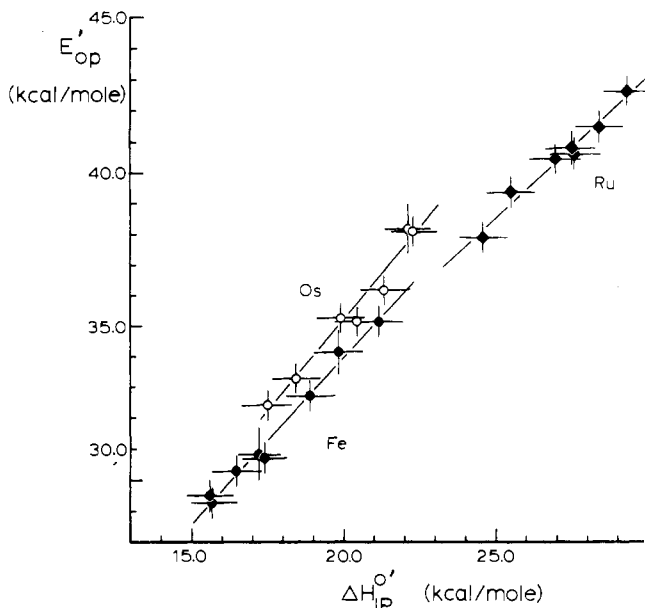


Figure 5. E_{op}' vs. $\Delta H_{IP}^{o'}$ where E_{op}' is the energy of the band maximum for the lower energy spin-orbit component.

tributions from the electron-donor and -acceptor sites. $\chi_{11i}/4$ and $\chi_{22i}/4$ are the classical, intramolecular vibrational trapping energies for the self-exchange reactions $M(CN)_6^{4-/3-}$ and $Ru(NH_3)_5(L)^{3+/2+}$. With the assumption that only the symmetric metal-ligand breathing modes make a significant contribution, χ_{11} is given by eq 16. In eq 16, k^{Red} and k^{Ox}

$$\chi_{11,inner} = 3(k^{Red} + k^{Ox})\Delta^2 \quad (16)$$

are the force constants for the symmetric breathing modes of one of the reactants in its reduced and oxidized forms and Δ is the difference in equilibrium metal-ligand bond distances for the normal mode in the two oxidation states.²⁸ For the specific case of the ferro-/ferricyanide self-exchange, $k^{Red} = k(Fe^{II}(CN)_6) = 2.4$ mdyne \AA^{-1} ,³² $k^{Ox} = k(Fe^{III}(CN)_6) = 2.4$ mdyne \AA^{-1} ,³³ and $\Delta = 0.026$ \AA ,^{24,26} leading to $\chi_{11} = 1.4$ kcal/mol.

When combined with the estimate $\chi_{22i} = 4.0$ kcal/mol for the $Ru(NH_3)_5(L)^{3+/2+}$ couple by Creutz,⁴ and Brown and Sutin,²⁸ $\chi_i = 2.7$ kcal/mol. Similar values for χ_i are expected for all of the ion pairs $[Fe^{II}(CN)_6, (NH_3)_5Ru^{III}(L)]^-$. For the corresponding osmium and ruthenium ion pairs, it is not possible to calculate χ_i because of the absence of structural and vibrational data for the $M^{III}(CN)_6^{3-}$ ions.

The calculated value of χ_i is relatively small compared to the total values of χ obtained from the intercepts of plots of E_{op}' vs. $\Delta H_{IP}^{o'}$ in Figure 5 (10–16 kcal/mol). The remainder of the total must come from χ_0 . A theoretical value for χ_0 can be calculated from eq 17, which is based on a dielectric

$$\chi_0 = e_0^2 \left(\frac{1}{2r_1} + \frac{1}{2r_2} - \frac{1}{d} \right) \left(\frac{1}{D_{op}} - \frac{1}{D_s} \right) \quad (17)$$

continuum model.^{3,7} In eq 17 e_0 is the unit electron charge, r_1 and r_2 are the radii of the reactants, d is the contact distance previously discussed, D_{op} is the square of the refractive index, and D_s is the bulk static dielectric constant. For water at 25 °C $D_{op} = 1.7756$ and $D_s = 78.54$,¹⁸ and using 4.5 \AA for $r(Fe(CN)_6^{4-})$, 4.3 \AA for $r((NH_3)_5Ru(py)^{3+})$, and $d = 8.3$ \AA gives $\chi_0 = 19.5$ kcal/mol, which is in only fair agreement with the experimental values suggested by the data in Figure 5: χ_0

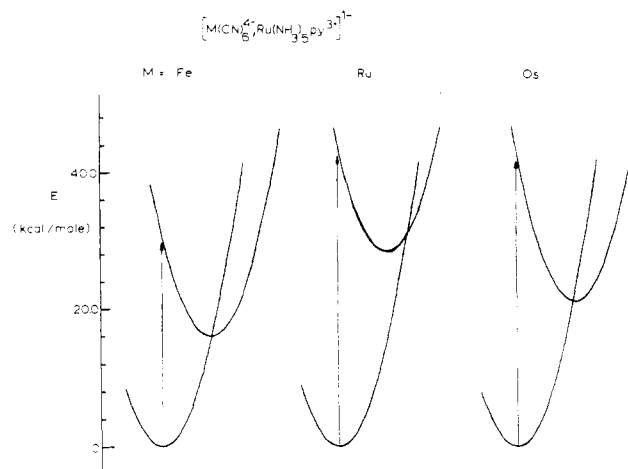


Figure 6. Potential energy surfaces for the ion pairs $[M^{II}(CN)_6, (NH_3)_5Ru^{III}py]^-$ ($M = Fe, Ru, Os$) and the high-energy redox isomers $[M^{III}(CN)_6, (NH_3)_5Ru^{II}py]^-$.

$= 7.4$ – 12.8 kcal/mol. The failure of eq 17 to make a reasonable prediction for χ_0 suggests a breakdown in the dielectric continuum model which has been shown to work well for large, mixed-valence ions where specific solvent effects are unimportant.⁴⁻⁷ A similar observation has been made recently for metal to ligand charge-transfer bands for ammine complexes where strong, specific hydrogen-bonding effects are known to be of importance.³⁴

Potential Energy Surfaces. With the data now available for the ion pairs, it is possible to map out their spectroscopic potential energy surfaces. In the limit of harmonic oscillator potential functions and equal force constants in both initial and final states, the intersection between the ground- and high-energy redox isomeric states is given by the classical activation energy in eq 18. Recall that χ is obtainable by using eq 19.^{3,5,8}

$$E_a = (\chi/4)(1 + (\Delta H_{IP}^{o'}/\chi))^2 \quad (18)$$

$$\chi = E_{op} - \Delta H_{IP}^{o'} \quad (19)$$

With the values for E_{op} and $H_{IP}^{o'}$ from Figure 5, the potential energy surfaces which result from eq 18 are shown in Figure 6 for the ion pairs $[M^{II}(CN)_6^{4-}, (NH_3)_5Ru^{III}py^{3+}]^-$, where, once again, harmonic oscillators and equal force constants for the upper and lower surfaces are assumed.

As can be seen from the figure, the diagrams are revealing in that all three systems appear to be hovering just at or are into the enthalpic analogue of the "abnormal free energy" region of Marcus' theory.³⁵ In this context it is useful to define three limits: $|\Delta H_{IP}^{o'}| < \chi$, the normal region where the reverse electron transfer $[M^{III}(CN)_6, Ru^{II}(NH_3)_5(py)]^- \rightarrow [M^{II}(CN)_6, Ru^{III}(NH_3)_5py]^-$ would involve thermal activation to the classical intersection between surfaces; $|\Delta H_{IP}^{o'}| = \chi$, for which no activation is required; $|\Delta H_{IP}^{o'}| > \chi$, the two potential surfaces are now "nested" and back electron transfer becomes a nonradiative photophysical process in the parlance of radiationless decay theory. When E_{op}' is considered, with our estimates for the spectroscopic energy of the lower spin-orbit states, all three cases shown in Figure 6 are well within the excited state domain.

Structure and Electronic Coupling within the Ion Pairs. From the results of a first-order perturbation treatment, Hush has derived eq 20.³ In eq 20 ϵ_{max} is the maximum extinction

$$\alpha^2 = (4.24 \times 10^{-4} \epsilon_{max} \Delta \bar{\nu}) / d^2 \bar{\nu}_{max} \quad (20)$$

(32) Deak, A.; Templeton, J. L. *Inorg. Chem.* **1980**, *19*, 1075.

(33) Sharpe, A. G. "The Chemistry of the Cyano Complexes of Transition Metals"; Academic Press: New York, 1976.

(34) Curtis, J.; et al., submitted for publication.

(35) Marcus, R. A. *J. Chem. Phys.* **1965**, *43*, 2654.

coefficient, $\Delta\bar{\nu}$ is the band width at half-height, $\bar{\nu}$ is the band energy maximum, and d is the distance in Å. The extent of electronic coupling or resonance energy β arising from orbital mixing is given simply by eq 21.

$$\beta = H_{12} = E_{op}\alpha \quad (21)$$

Values of α^2 and β are included for all of the ion pairs in Table IV. As can be seen from the table, the values of α^2 for the ion pairs involving ferro- and ruthenocyanide are essentially the same, 1.09×10^{-4} and 1.08×10^{-4} , respectively, and an average value for the osminocyanide ion pairs is higher at 1.42×10^{-4} . This increase seems rather modest given the steady increase in the d orbital extension within the series Os > Ru > Fe.

This seeming paradox of a nearly metal-independent value for α^2 strongly supports the importance of metal-ligand mixing in determining the magnitude of electronic coupling in outer-sphere electron transfer. If there were significant interpenetration of coordination spheres and significant metal-metal overlap, a more dramatic metal-based dependence of α^2 should have been observed.

The average values of the resonance energy β increase steadily but not remarkably within the series ferro- to ruthenocyanide. In all cases the interaction energy is sufficiently large ($100\text{--}200\text{ cm}^{-1}$) that the corresponding thermal electron-transfer reactions are near the adiabatic regime, in the semiclassical view—that is, that the probability of surface crossing at the intersection is close to unity.³⁶

Our work provides strong evidence in support of the notion that at least for the ion pairs that we detect optically, the structure involves the ammine face of $\text{Ru}(\text{NH}_3)_5(\text{L})^{3+}$ ion. There are two bases for this statement. One is that the energies of intervalence-transfer absorption bands have been shown to be a sensitive function of the distance between the interacting redox sites.²² Since the OSCT band energies in the ion pairs correlate well with H_{1p}° and are not appreciably affected by bulky substituents on the ligand L, it seems reasonable to conclude that the optical interaction must of necessity be occurring over the same distance of all of the ion pairs of a given series. The low-energy pathway for thermal electron transfer is also probably through the ammonia ligands rather than the nitrogen heterocyclic, given the predictions made elsewhere concerning distance dependencies.²²

Miralles et. al have proposed that the pyridine ligand provides the important conductive pathway in the outer-sphere, thermal reduction of pentammine(pyridine) ruthenium(III)

by ferrocyanide as shown in eq 6. They base their arguments on the subtle numerical effects of the two alternate distances involved (transfer through pyridine or ammonia) on the calculated electrostatic work terms $Z_1Z_2e_0^2/D_s d$ and the fact that the π^* orbitals on the ligand are of proper symmetry to deliver an incoming electron to the unfilled t_{2g} orbital of the d^5 ruthenium(III) center. However, Miralles et. al did not consider in their analysis the distance dependence expected in χ_0 , and their conclusions are not valid.

A second consideration to note is the near constancy of α^2 values through the series of cations $\text{Ru}(\text{NH}_3)_5(\text{L})^{3+}$ for all three of the hexacyano ions. In the end, the magnitude of α will be determined by a series of overlap-type integrals which will be strongly dependent on the distance between the electron-donor and -acceptor sites. The near constancy of α through the series argues strongly for a common outer-sphere "structure" at least in the sense of the electronic interaction being along an ammine face rather than along a face including the pyridine ligand.

Acknowledgments are made to the National Science Foundation for support of this research.

Registry No. $\text{K}_4[\text{Fe}(\text{CN})_6]$, 13943-58-3; $\text{K}_4[\text{O}_5(\text{CN})_6]$, 20740-36-7; $\text{K}_4[\text{Ru}(\text{CN})_6]$, 15002-31-0; $[\text{Ru}(\text{NH}_3)_6]\text{Cl}_3$, 14282-91-8; $[(\text{NH}_3)_5\text{Ru}(\text{Im})]\text{Cl}_3$, 51982-73-1; $[(\text{NH}_3)_5\text{Ru}(\text{Me}_2\text{pzl})]\text{Cl}_3$, 80584-08-3; $[(\text{NH}_3)_5\text{Ru}(\text{pzl})]\text{Cl}_3$, 80584-09-4; $[(\text{NH}_3)_5\text{Ru}(4\text{-Mepy})]\text{Cl}_3$, 80584-10-7; $[(\text{NH}_3)_5\text{Ru}(4\text{-}i\text{-Bupy})]\text{Cl}_3$, 80584-11-8; $[(\text{NH}_3)_5\text{Ru}(\text{py})]\text{Cl}_3$, 80584-12-9; $[(\text{NH}_3)_5\text{Ru}(4\text{-Cl}(\text{py}))]\text{Cl}_3$, 80584-13-0; $[(\text{NH}_3)_5\text{Ru}(4\text{-Br}(\text{py}))]\text{Cl}_3$, 80584-14-1; $[(\text{NH}_3)_5\text{Ru}(3\text{-Cl}(\text{py}))]\text{Cl}_3$, 80593-40-4; $[(\text{NH}_3)_5\text{Ru}(3,5\text{-Cl}_2(\text{py}))]\text{Cl}_3$, 80593-41-5; $[(\text{NH}_3)_5\text{Ru}(\text{Me}_2\text{pyz})]\text{Cl}_3$, 80593-42-6; $\text{Li}[\text{trans}(\text{py})\text{Ru}(\text{NH}_3)_4\text{NCRu}(\text{CN})_5]$, 80679-04-5; $[\text{Fe}^{\text{II}}(\text{CN})_6, \text{Ru}^{\text{III}}(\text{NH}_3)_5(4\text{-Br}(\text{py}))]^-$, 80593-44-8; $[\text{Fe}^{\text{II}}(\text{CN})_6, \text{Ru}^{\text{III}}(\text{NH}_3)_5(4\text{-Cl}(\text{py}))]^-$, 80593-45-9; $[\text{Fe}^{\text{II}}(\text{CN})_6, \text{Ru}^{\text{III}}(\text{NH}_3)_5(\text{py})]^-$, 68168-01-4; $[\text{Fe}^{\text{II}}(\text{CN})_6, \text{Ru}^{\text{III}}(\text{NH}_3)_5(4\text{-Mepy})]^-$, 80593-46-0; $[\text{Fe}^{\text{II}}(\text{CN})_6, \text{Ru}^{\text{III}}(\text{NH}_3)_5(4\text{-}i\text{-Bupy})]^-$, 80593-47-1; $[\text{Fe}^{\text{II}}(\text{CN})_6, \text{Ru}^{\text{III}}(\text{NH}_3)_5(\text{pzl})]^-$, 80593-49-3; $[\text{Fe}^{\text{II}}(\text{CN})_6, \text{Ru}^{\text{III}}(\text{NH}_3)_5(\text{Mepzl})]^-$, 80593-51-7; $[\text{Fe}^{\text{II}}(\text{CN})_6, \text{Ru}^{\text{III}}(\text{NH}_3)_5(\text{Im})]^-$, 80593-53-9; $[\text{Ru}^{\text{II}}(\text{CN})_6, \text{Ru}^{\text{III}}(\text{NH}_3)_5(\text{Me}_2\text{pyz})]^-$, 80593-55-1; $[\text{Ru}^{\text{II}}(\text{CN})_6, \text{Ru}^{\text{III}}(\text{NH}_3)_5(3,5\text{-Cl}_2(\text{py}))]^-$, 80593-56-2; $[\text{Ru}^{\text{II}}(\text{CN})_6, \text{Ru}^{\text{III}}(\text{NH}_3)_5(3\text{-Cl}(\text{py}))]^-$, 80593-57-3; $[\text{Ru}^{\text{II}}(\text{CN})_6, \text{Ru}^{\text{III}}(\text{NH}_3)_5(4\text{-Br}(\text{py}))]^-$, 80593-58-4; $[\text{Ru}^{\text{II}}(\text{CN})_6, \text{Ru}^{\text{III}}(\text{NH}_3)_5(4\text{-Cl}(\text{py}))]^-$, 80593-59-5; $[\text{Ru}^{\text{II}}(\text{CN})_6, \text{Ru}^{\text{III}}(\text{NH}_3)_5(\text{py})]^-$, 80593-60-8; $[\text{Ru}^{\text{II}}(\text{CN})_6, \text{Ru}^{\text{III}}(\text{NH}_3)_5(4\text{-Mepy})]^-$, 80593-61-9; $[\text{Os}^{\text{II}}(\text{CN})_6, \text{Ru}^{\text{III}}(\text{NH}_3)_5(\text{Me}_2\text{pyz})]^-$, 80593-62-0; $[\text{Os}^{\text{II}}(\text{CN})_6, \text{Ru}^{\text{III}}(\text{NH}_3)_5(3,5\text{-Cl}_2(\text{py}))]^-$, 80593-63-1; $[\text{Os}^{\text{II}}(\text{CN})_6, \text{Ru}^{\text{III}}(\text{NH}_3)_5(4\text{-Br}(\text{py}))]^-$, 80593-64-2; $[\text{Os}^{\text{II}}(\text{CN})_6, \text{Ru}^{\text{III}}(\text{NH}_3)_5(3\text{-Cl}(\text{py}))]^-$, 80584-15-2; $[\text{Os}^{\text{II}}(\text{CN})_6, \text{Ru}^{\text{III}}(\text{NH}_3)_5(\text{py})]^-$, 80584-16-3; $[\text{Os}^{\text{II}}(\text{CN})_6, \text{Ru}^{\text{III}}(\text{NH}_3)_5(4\text{-}i\text{-Bupy})]^-$, 80584-18-5; $[\text{Os}^{\text{II}}(\text{CN})_6, \text{Ru}^{\text{III}}(\text{NH}_3)_5(4\text{-Mepy})]^-$, 80584-20-9; $[\text{Fe}^{\text{III}}(\text{CN})_6, \text{Ru}^{\text{II}}(\text{NH}_3)_5(\text{py})]^-$, 80584-21-0; $[\text{Ru}^{\text{III}}(\text{CN})_6, \text{Ru}^{\text{II}}(\text{NH}_3)_5(\text{py})]^-$, 80584-22-1; $[\text{Os}^{\text{III}}(\text{CN})_6, \text{Ru}^{\text{II}}(\text{NH}_3)_5(\text{py})]^-$, 80584-23-2; $[(\text{NH}_3)_5\text{Ru}^{\text{III}}\text{Cl}]\text{Cl}_2$, 18532-87-1; $[\text{trans-pyRu}^{\text{III}}(\text{NH}_3)_4\text{SO}_4]\text{Cl}$, 80584-24-3.

(36) Brunshwig, B.; Logan, J.; Newton, M. D.; Sutin, N. *J. Am. Chem. Soc.* **1980**, *102*, 5798.